SUPPLEMENTARY DATA

Analysis of Pdx-1 Cre recombinase activity

Pdx-1 Cre recombinase activity was examined by crossing *Pdx-1Cre*$^{+/-}$ mice to tdTomato reporter mice. We detected Cre-mediated tdTomato expression in the pancreas, but also in duodenum and liver at different embryonic and postnatal stages (Supplementary Fig. 3.1K-DD). In embryonic and early postnatal pancreas development MANF was found to be expressed in most cells with the highest expression in endocrine cells (Supplementary Fig. 3.1K-M, O-Q).

Pancreas-specific ablation of MANF leads to diabetes in mice

The absence of MANF from conventional *Manf* $^{-/-}$ mice and from the pancreases of conditional *Pdx-1Cre*$^{+/-}$::*Manf*$^{fl/fl}$ mice results in diabetes (1). In contrast to *Manf*$^{-/-}$ mice, the *Pdx-1Cre*$^{+/-}$::*Manf*$^{fl/fl}$ mice do not show growth retardation (Supplementary Fig. 2.1B), suggesting that MANF-removal from other cells rather than β-cells results in the growth defect in conventional *Manf*$^{-/-}$ mice. A slight reduction in weight was observed in P56 *Pdx-1Cre*$^{+/-}$::*Manf*$^{fl/fl}$ mice, when animals already were overtly diabetic. In contrast to *Manf*$^{-/-}$ mice, *Pdx-1Cre*$^{+/-}$::*Manf*$^{fl/fl}$ mice developed diabetes later. Blood glucose and serum insulin levels were within the normal range in P1 and P14 random fed animals (Supplementary Fig. 2.1C-D). However, severe hyperglycaemia and significant reduction in serum insulin levels were observed in random fed P56 conditional mice (Supplementary Fig. 2.1C-D). Glucose tolerance test revealed impaired glucose clearance and a trend toward reduced glucose stimulated insulin secretion in P56 *Pdx-1Cre*$^{+/-}$::*Manf*$^{fl/fl}$ compared to controls (Supplementary Fig. 2.1E-F). As reported for *Manf*$^{-/-}$ mice (1), insulin tolerance test performed on P42 *Pdx-1Cre*$^{+/-}$::*Manf*$^{fl/fl}$ conditional mice revealed intact insulin sensitivity (Supplementary Fig. 2.1G).

Histological analysis of pancreases revealed marked loss of islet architecture and reduced insulin staining in P56 *Pdx-1Cre*$^{+/-}$::*Manf*$^{fl/fl}$ mice (Supplementary Fig. 2.1I-N, 2.1O-T). Quantification of the β-cell mass demonstrated no changes at P1. However, by P14 the β-cell mass was reduced in *Pdx-1Cre*$^{+/-}$::*Manf*$^{fl/fl}$ pancreases compared to controls (Supplementary Fig. 2.1U). Consequently, islet-cell mass in P56 *Pdx-1Cre*$^{+/-}$::*Manf*$^{fl/fl}$ pancreases was reduced (data not shown), indicating β-cell loss. Consistent with our data with global *Manf*$^{-/-}$ mice, lack of MANF from the pancreas resulted in a significantly reduced number of Ki67 positive β-cells starting at P14 (Supplementary Fig. 2.1W). The reduction of the β-cell mass was also accompanied by increased levels of β-cell apoptosis in P14 and P56 pancreases from conditional mice quantified by TUNEL assay (Supplementary Fig. 2.1X, 2.1Y-DD).

Supplemental Experimental Procedures

Animals and in vivo physiology

In brief, *Manf*$^{fl/fl}$ mice were produced by removing the β-galactosidase reporter cassette preceded by a strong splicing acceptor by crossing *Manf*$^{+/-}$ mice with ubiquitous Flp expressing *CagFlp* mice (1) and (Supplementary Fig. 2.1A).

Pdx-1Cre recombinase activity was evaluated by crossing *Pdx-1Cre* mice with *Rosa26-tdTomato*$^{fl/Stop/fl}$ reporter mice (Jackson Laboratories, Stock 007914).

Collected blood samples from the mice were assayed for glucose (Accucheck Aviva Glucometer; Roche Diagnostics) and sera for insulin (ultrasensitive mouse insulin ELISA; Crystal Chem) measurements. DNA isolation and genotyping of mice were carried out as described previously (1,2) and in Supplementary Data.

Genotyping primers and expected PCR products

DNA was isolated from ear-marks and genotyping was carried out. For *MIP-1Cre*^{ERT} mice the following primers were used: Forward (transgene) 5'-TGGACTATAAAGCTGGTGGGCAT-3', Reverse (transgene) 5'-TGCGAACCTCATCACTCGT-3', Internal Positive Control Forward 5'-CTAGGCCACAGAATTGAAAGATCT-3', Internal Positive Control Reverse 5'-GTAGGTGGAAATTCTAGCATCATCC-3' (PCR products: Transgene = ~230 bp, Internal positive

control = 324 bp). For *Rosa26-tdTomato*$^{fl/Stop/fl}$ reporter mice the following primers were used: Wild type Forward 5'-AAGGGA GCT GCA GTG GAG TA-3', Wild type Reverse 5'-CCG AAA ATC TGT GGG AAG TC-3', Mutant Reverse 5'-GGCATTAAAGCAGCGTATCC-3', Mutant Forward 5'-CTGTTCCTG TACGGCATGG-3' (PCR products: Mutant = 196 bp, Heterozygote = 297 bp and 196 bp, Wild type = 297 bp).

Histological Analysis

Islet-cell mass was assessed from pancreatic sections stained with anti-Chromogranin A antibody and quantified similarly to beta cell mass described previously (1).

For identification of LacZ activity cryosections were stained with X-gal solution as described previously (3).tdTomato expression was detected in cryosections as described previously (4) and followed by staining with anti-MANF antibody and DAPI.

Fluorescence or light microscopy images were captured with 3DHISTECH Panoramic 250 FLASH II digital slide scanner (Budapest, Hungary, with scanning service in the Institute of Biotechnology and in Research Programs Unit, Faculty of Medicine, University of Helsinki, Biocenter Finland) or Zeiss AxioImager M2 482 epifluorescence microscope equipped with 483 AxioCam HRm camera. Images were analysed with Pannoramic viewer program or acquired with the AxioVision4 software.

Subcellular localization analysis

Islets from C57BL/6Rcc pancreases were isolated and cultured overnight in the RPMI1649 medium supplemented with 10% Fetal Bovine Serum and a mixture of antibiotics. Next day islets were dissociated with Tryple^{TM} Select Enzyme (Cat.number 12563011, Thermo Fisher Scientific, Waltham MA, USA), followed by centrifugation onto glass slides. Cells were fixed and stained for different primary antibodies (Supplementary Table 1). Appropriate secondary antibodies conjugated with Alexa Fluor® 488 or 568 (1:400, Molecular Probes, Life Technologies, Eugene, Oregon, USA) and DAPI (Vectorshield, Vector laboratories, Burlingame, USA) were used to visualize the labels.

Slides were imaged with PerkinElmer Opera Phenix high-content confocal microscope using Harmony 4.6 software (PerkinElmer), by using three lasers with excitation wavelengths 405nm, 488nm, and 568nm. 63x water immersion objective (NA 1.15) was used for imaging. The lateral pixel size was automatically set to 95nm and the distance between axial slices was set to 500nm according to the Nyquist criterion. Altogether 10-14 optical sections were recorded using 16-bit Andor Zyla CMOS camera (2160x2160 px). 125 and 49 fields-of-view were recorded from the first and second set of slides, respectively.

The colocalization analysis was performed in 3D for each cell separately. Densely packed and malformed cells were filtered out from the analysis. First, nuclei and cells were segmented from 2D maximum intensity projection images using Harmony software. Next, linear classifier was trained to classify cells into two classes: isolated and packed/malformed. Last, the 2D coordinates of isolated cells were exported from Harmony software. The rest of the analysis was carried out in 3D using BioImageXD software (5). Cells were segmented in 3D using combination of Hoechst and MANF (568nm) channels. Only the cells overlapping with the exported 2D coordinates of isolated cells were used for colocalization analysis. For each cell, both Pearson correlation coefficient for overall signal correlation and Manders' coefficients (6) for channel specific colocalization were measured. The total number of analysed cells varied from 20 to 66.

Western Blotting

Western blotting analysis was performed using standard protocols and as described previously (1). For primary antibodies see Supplementary Table 1.

Islet isolation, In Vitro Insulin Release and In Vitro Islets experiments

SUPPLEMENTARY DATA

Islet isolation and *in vitro* insulin release from islets were performed as described previously (1,7). In brief, pancreases were digested by collagenase P (Collagenase P; Roche Diagnostics) using standard protocol procedure and islets were purified from acinar tissues by handpicking them up under a microscope.

In order to test the effect of human recombinant MANF on ER stress in MANF-deficient islets we cultured isolated islets from 4-5-week old *Manf*$^{+/+}$ and *Manf*$^{-/-}$ mice for 24 h with or without MANF (1µg/ml, Icosagen) in 0.5% bovine serum albumin (BSA) in RPMI medium directly after islets isolation or with MANF (100ng/ml, Icosagen) for 3 days in 10% FBS RPMI medium, changing 2/3 of the medium into fresh every day.

To test the effect of MANF on mouse islets exposed to hyperglycaemia, isolated islets from 12- week-old C57BL/6Rcc mice were cultured in RPMI medium (glucose 11mM) supplemented with 0.5% BSA in the presence and absence of high levels of glucose (30mM) overnight with or without MANF 1µg/ml.

Analysis of Blood Samples by glucose tolerance test (GTT), insulin tolerance test (ITT), and by glucose challenge test (GTT).

Analysis of blood samples were performed as described previously (1).

RNA Isolation, Reverse Transcription, and Quantitative RT-PCR

RNA Isolation, reverse transcription, and quantitative real-time polymerase chain reaction (QPCR) were performed as described previously (1). Primer sequences for the gene expression studied by QPCR have been described previously (1). Other primer sequences: *mouse Bcl10* Forward 5'-AAA CTG GAG CAC CTC AAA GG -3', *mouse Bcl10* Reverse 5'-TCT CAT CGG AAT TGC ACC TA -3', *mouse Trib3* Forward 5'- CGC TTT GTC TTC AGC AAC TGT-3', *mouse Trib3* Reverse 5'-TCA TCT GAT CCA GTC ATC ACG -3'.

Serial block-face scanning electron microscopy (SB-EM)

The dissected tissues (<2 mm x 2 mm blocks) were stained using an enhanced staining protocol (8). First, the tissues were fixed with 2.5% glutaraldehyde and 2% formaldehyde, in 100 mM Na-cacodylate buffer (pH 7.4) supplemented with 2 mM $CaCl_2$ for 2 hours. Stained and dehydrated specimens were embedded into Durcupan ACM resin (Merck Sigma-Aldrich, Darmstadt, Germany), that was mixed according to the manufacturer's recommendations. The embedded tissue was trimmed to a pyramid and mounted onto a pin using conductive epoxy glue (model 2400; CircuitWorks, Kennesaw, GA). Finally, the sides of the pyramid were covered with silver paint (Agar Scientific Ltd, Stansted, UK), and the whole assembly was platinum coated using Quorum Q150TS (Quorum Technologies, Laughton, UK). SBEM data sets were acquired with an FEG-SEM Quanta 250 (Thermo Fisher Scientific, FEI, Hillsboro, OR), using a backscattered electron detector (Gatan Inc., Pleasanton, CA) with 2.5-kV beam voltage, a spot size of 3, and a pressure of 0.15-0.30 Torr. The block faces were cut with 40-nm increments and imaged with XY resolution of 16 nm per pixel.

References

1. Lindahl M, Danilova T, Palm E, Lindholm P, Voikar V, Hakonen E, Ustinov J, Andressoo JO, Harvey BK, Otonkoski T, Rossi J, Saarma M: MANF is indispensable for the proliferation and survival of pancreatic beta cells. Cell Rep 2014;7:366-375

2. Tamarina NA, Roe MW, Philipson L: Characterization of mice expressing Ins1 gene promoter driven CreERT recombinase for conditional gene deletion in pancreatic beta-cells. Islets 2014;6:e27685

3. Aird WC, Jahroudi N, Weiler-Guettler H, Rayburn HB, Rosenberg RD: Human von Willebrand factor gene sequences target expression to a subpopulation of endothelial cells in transgenic mice. Proc Natl

SUPPLEMENTARY DATA

Acad Sci U S A 1995;92:4567-4571
4. Morris LM, Klanke CA, Lang SA, Lim FY, Crombleholme TM: TdTomato and EGFP identification in histological sections: insight and alternatives. Biotech Histochem 2010;85:379-387
5. Kankaanpää P, Paavolainen L, Tiitta S, Karjalainen M, Päivärinne J, Nieminen J, Marjomäki V, Heino J, White DJ: BioImageXD: an open, general-purpose and high-throughput image-processing platform. Nature Methods 2012;9:683
6. Manders EMM, Verbeek FJ, Aten JA: Measurement of Colocalization of Objects in Dual-Color Confocal Images. J Microsc-Oxford 1993;169:375-382
7. Miettinen PJ, Ustinov J, Ormio P, Gao R, Palgi J, Hakonen E, Juntti-Berggren L, Berggren PO, Otonkoski T: Downregulation of EGF receptor signaling in pancreatic islets causes diabetes due to impaired postnatal beta-cell growth. Diabetes 2006;55:3299-3308
8. Deerinck TJ, Bushong E, Thor A. Ellisman MH. NCMIR methods for 3D EM: A new protocol for preparation of biological specimens for serial block-face SEM. Microscopy. 2010:6–8. https://ncmir.ucsd.edu/sbem-protocol

SUPPLEMENTARY DATA

Supplementary Figure 1.1. supporting Figure 1. MANF is specifically expressed in the β-cell of the islets of Langerhans.

Detection of β-galactosidase activity under the control of MANF promoter in E12.5 pancreatic primordium and adult pancreas was detected by X-gal staining in *Manf*$^{+/-}$ heterozygote chimeric animals. **(A, B)** LacZ stained (blue) cryosections counterstained with nuclear fast red (pink) from *Manf* $^{+/-}$ chimeric embryo at E12.5 **(A)** and from adult *Manf* $^{+/-}$ chimeric pancreas **(B)**. Scale bar, 100 µm.
(C-D) Immunohistochemical localization of MANF protein in *Manf* $^{+/+}$ **(C)** and in *Manf* $^{-/-}$ **(D)** pancreas as negative control by using anti-ARP (MANF) antibody (Santa Cruz). Scale bar, 100 µm.
(E-J) Double immunohistochemistry analysis with MANF **(F, I)** GLUT2 **(E)**, and PDX1 **(H)**. Nearly all MANF positive cells (red) expressed GLUT 2 at the cell membrane of β-cells **(E-G)** whereas all MANF-positive cells showed nuclear staining for PDX1 (green) **(H-J)**. Cell nuclei were labelled with DAPI (blue). Scale bar, 10 µm.
(K-V) Representative confocal laser scanning microscopy images of double immunocytochemistry analysis of primary mouse β-cells using anti-MANF antibody (red) **(K-R)** with anti-PDI (Protein Disulphide Isomerase, ER marker, green) **(K, S)**, anti-GM130 (Golgi marker, green) **(L, T)**, anti-insulin (green) **(M, U)** and anti-GRP78 (green) **(N, V)** antibodies. Scale bar, 8 µm.

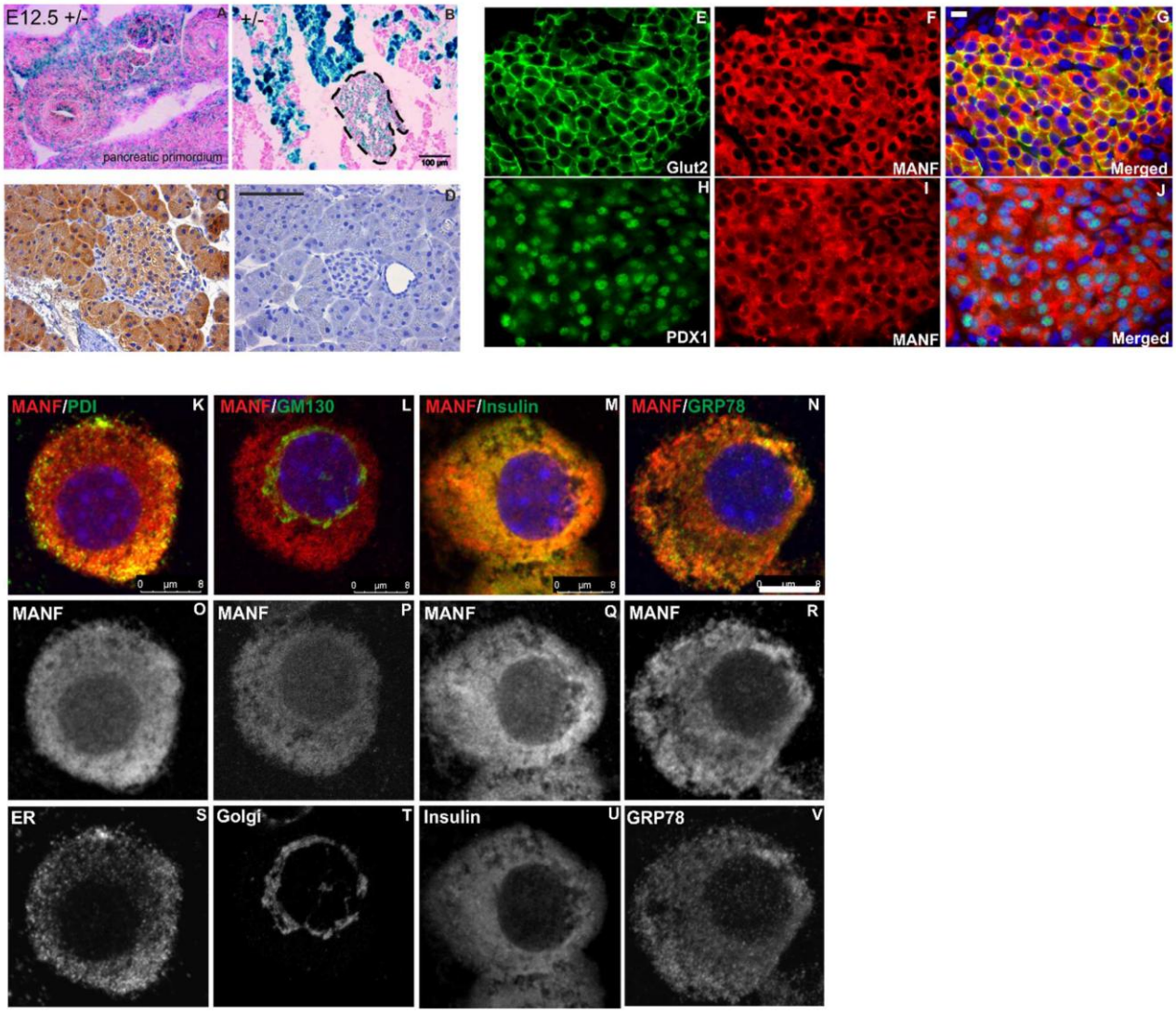

SUPPLEMENTARY DATA

Supplementary Figure 1.2. supporting Figure 1. MANF expression in the β-cells of diabetic mouse models NOD and db/db.

(A-F) MANF **(A, D),** insulin **(B, E)** and glucagon **(C, F)** immunohistochemistry on pancreas sections from 11-week-old NOR (A, B, C) and NOD (D, E, F) mice. Scale bar, 20 µm.

(G-L) Double immunohistochemistry on pancreatic sections from 11-week-old NOR and NOD mice with anti-MANF (green) **(G, J)** and anti-insulin antibodies (red) **(H, K)** show increased MANF expression in β-cells in the periphery of islets near lymphocytic inflammatory cells invading the islets. Cell nuclei in merged pictures **(I, L)** labelled with DAPI (blue). Scale bar, 50µm.

(M-S) MANF **(M, Q),** insulin **(N, R)** and glucagon **(O, S)** immunohistochemistry on pancreas sections from 8-week-old db/+ **(M, N, O)** and db/db **(Q, R, S)** mice. Scale bar, 20 µm.

(T-Y) Double immunohistochemistry with anti-MANF (green) **(T, W)** and anti-insulin antibodies (red) **(U, X)** revealed disturbed islet architecture (W, X) and increased expression of MANF in some db/db islet β-cells (X) whereas others appeared to have reduced expression compared to MANF-stained β-cells in the control db/+ islets in 8-week-old mice. Cell nuclei in merged picture **(V, Y)** labelled with DAPI (blue). Scale bar, 50µm.

SUPPLEMENTARY DATA

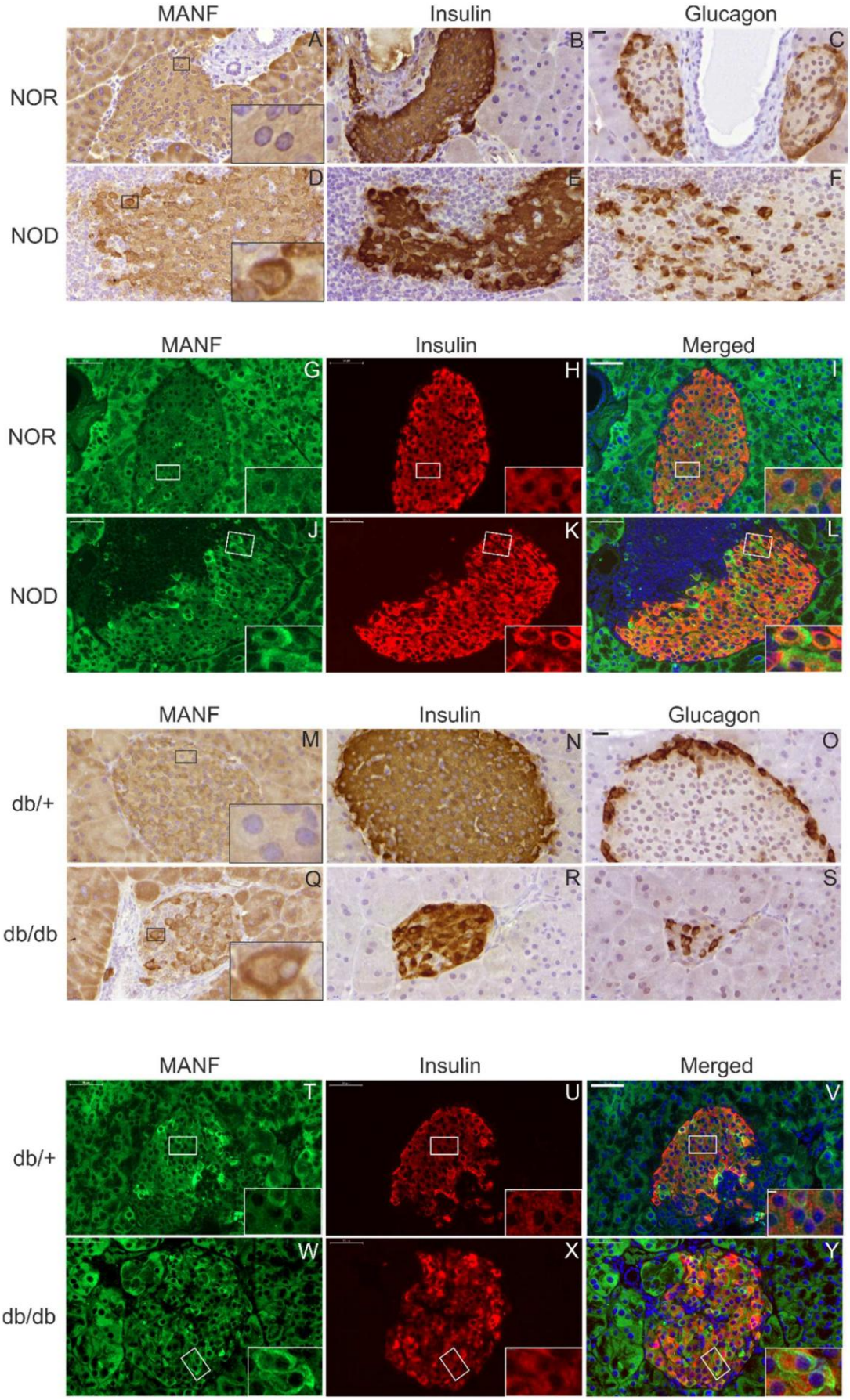

SUPPLEMENTARY DATA

Supplementary Figure 2.1. supporting Figure 2. Absence of MANF in pancreas results in diabetes in *Pdx-1Cre*$^{+/-}$::*Manf*$^{fl/fl}$ mice.

(A) Schematic representation of the *Manf*$^{+/+}$wild-type, *Manf*$^{-/-}$, *Manf*$^{flox/flox(fl/fl)}$ and *Cre*::*Manf* $^{fl/fl}$ targeted allele. The strong splice-acceptor and β-galactosidase cassette was removed by crossing of *Manf* $^{+/-}$ to *CAG-Flp* transgenic mice in order to produce *Manf*$^{fl/fl}$ mice, where exon 3 is flanked with LoxP sites enabling removal in Cre-expressing cells. β-galactosidase reporter cassette (β-gal), strong splicing acceptor site (En2SA), exon (E), Frt (F)-sites, LoxP (L)-sites, βAct::Neo; human β-actin promoter driven neomycin resistance gene.

(B) Growth curve of *Manf*$^{fl/fl}$ and *Pdx-1Cre*$^{+/-}$::*Manf*$^{fl/fl}$ littermates. P1–P56, *n* =5-18 per group, combined from both sexes.

(C) Ad libitum-fed blood glucose levels, *n*=9-21 per group;

(D) Serum insulin levels from ad libitum-fed mice, *n* = 9–15 per group;

(E) Blood glucose levels measured after intraperitoneal glucose (2 g/kg) injection, *n* =8-9 mice per group.

(F) Serum insulin levels in P56 mice measured 30 min after glucose (2 g/kg) bolus injection, *n* =7 mice per group.

(G) Blood glucose levels measured after intraperitoneal injection of insulin (1 U/kg), *n* =7-8 mice per group.

(I-N) Insulin immunohistochemistry on pancreas sections from *Manf*$^{fl/fl}$ **(I-K)** and *Pdx-1Cre*$^{+/-}$::*Manf*$^{fl/fl}$ **(L-N)** animals at P1 **(I, L)**, P14 **(J, M)**, and P56 **(K, N)**. The scale bar represents 20 μm.

(O-T) Insulin **(O-Q)** and glucagon **(R-T)** immunohistochemistry on pancreas sections from P56 *Pdx-1Cre*, *Manf*$^{fl/fl}$ and *Pdx-1Cre*$^{+/-}$::*Manf*$^{fl/fl}$ mice. Scale bar, 50 μm.

(U) Reducedβ-cell mass in *Pdx-1Cre*$^{+/-}$::*Manf*$^{fl/fl}$ mice from P14, *n* = 6-20 per group.

(V) α-cell mass in *Pdx-1Cre*$^{+/-}$::*Manf*$^{fl/fl}$ mice, *n* = 5-7 per group.

(W) β-cell proliferation assessed by Ki67 and insulin staining, *n* =5-12 per group.

(X) β-cell apoptosis assessed by TUNEL and insulin staining, *n* =5-12 per group.

(Y-DD) Double immunohistochemistry on pancreas sections from *Manf*$^{fl/fl}$ and *Pdx-1Cre*$^{+/-}$::*Manf*$^{fl/fl}$ pancreases at P56 using TUNEL (green)- and anti-insulin (red) staining. Arrowheads point to TUNEL-positive β-cell (R). Scale bar 50 μm.

Values represent mean ± SEM, *p < 0.05, **p < 0.01, ***p< 0.001.

SUPPLEMENTARY DATA

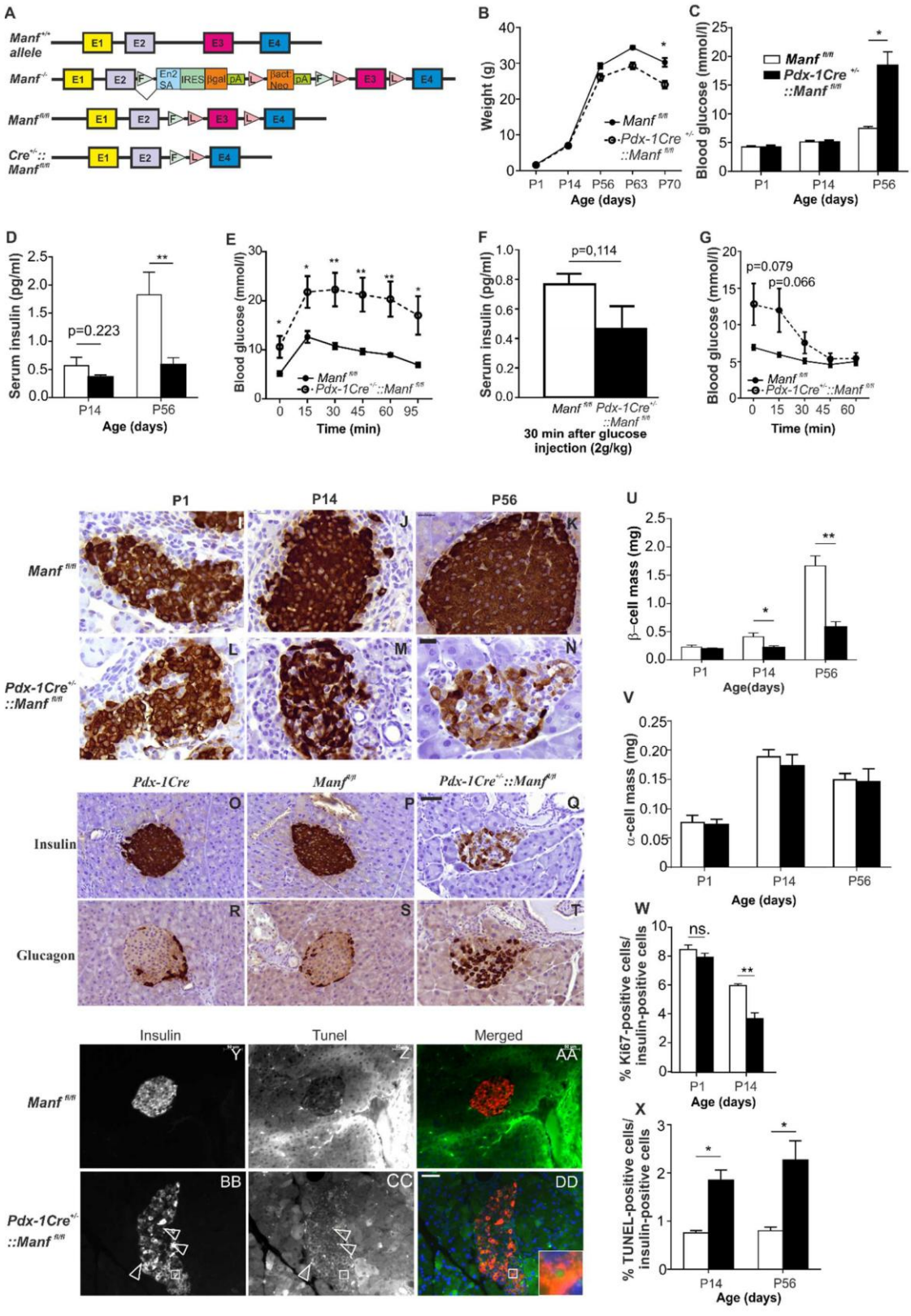

SUPPLEMENTARY DATA

Supplementary Figure 2.2. supporting Figure 2. Analysis of Pdx-1 Cre recombinase activity
(A-J) MANF immunohistochemistry on brain sections from *Manf*$^{fl/fl}$ **(A-E)** and *Pdx-1Cre*$^{+/-}$ ::*Manf*$^{fl/fl}$ mice **(F-J)**. No visible differences were observed in MANF expression in the cortex **(A, F)**, hippocampus **(B, G)**, paraventricular nuclei of hypothalamus (PVN) **(C, H)**, dorsal medial nuclei of hypothalamus (DMH) **(D-I)** and supraoptic nuclei of hypothalamus **(E, J)**. Scale bar, 50µm.
(K-R) Co-expression of MANF and tdTomato red fluorescent protein. Double immunohistochemistry analysis of MANF (green) and tdTomato (red) expression in the pancreases of *Pdx-1Cre*$^{+/-}$::*tdTomato* **(K-N)** and *tdTomato* mice **(O-R)**. dtTomato expression was observed in developing pancreatic primordium at E12.5, when high MANF signal was detected in some cells of the pancreatic primordium probably representing insulin-positive cells **(K)**. At E18.5 **(L)** Tomato expression was detected in the islet nuclei of MANF positive cell. At P3 **(M)** and P56 **(N)** Tomato expression was found in the nuclei of endocrine islets and in exocrine tissue mostly overlapping with MANF expression. However, some MANF-positive cells lacked Tomato expression, explaining the incomplete deletion of MANF from pancreas tissue leading to mosaic expression of MANF in *Pdx-1Cre*$^{+/-}$::*Manf*$^{fl/fl}$ mice. Notably, no Tomato signal was observed in the *tdTomato* mice lacking Cre, indicating that the system is not leaky **(O-R)**. Cell nuclei were labelled with DAPI (blue). Scale bar, 100 µm.
(J-Q) Merged pictures of double immunohistochemistry analysis with MANF and Tomato expression in the duodenum region of the intestine of *Pdx-1Cre*$^{+/-}$::*tdTomato* **(S-V)** and *tdTomato* mice **(W-Z)**. MANF and Tomato expression was observed in developing intestine at E12.5 **(S)**. At E18.5 **(T)**, P3 **(U)**, P56 **(V)** Tomato expression was detected in the villi of duodenum with mosaic expression pattern. Notably, no positive Tomato signal was observed in the *tdTomato* mice, indicating the specificity of the expression pattern in *Pdx-1Cre*$^{+/-}$::*tdTomato* **(W-Z)**. Cell nuclei were labelled with DAPI (blue). Scale bar, 100 µm.
(AA-DD) Merged pictures of double immunohistochemistry analysis with MANF and Tomato expression in the liver of *Pdx-1Cre*$^{+/-}$::*tdTomato* **(AA, BB)** and *tdTomato* mice **(CC, DD)**. Surprisingly, few positive Tomato cell were detected in the liver of P3 **(AA)** and P56 **(BB)** in *Pdx-1Cre*$^{+/-}$::*tdTomato*. However, no positive Tomato expression was observed in E18.5 **(R, U).** Notably, no positive Tomato signal was observed in the *tdTomato* mice, indicating the specificity of the expression pattern in *Pdx-1Cre*$^{+/-}$::*tdTomato* **(CC, DD)**. Cell nuclei were labelled with DAPI (blue). Scale bar, 100 µm.

SUPPLEMENTARY DATA

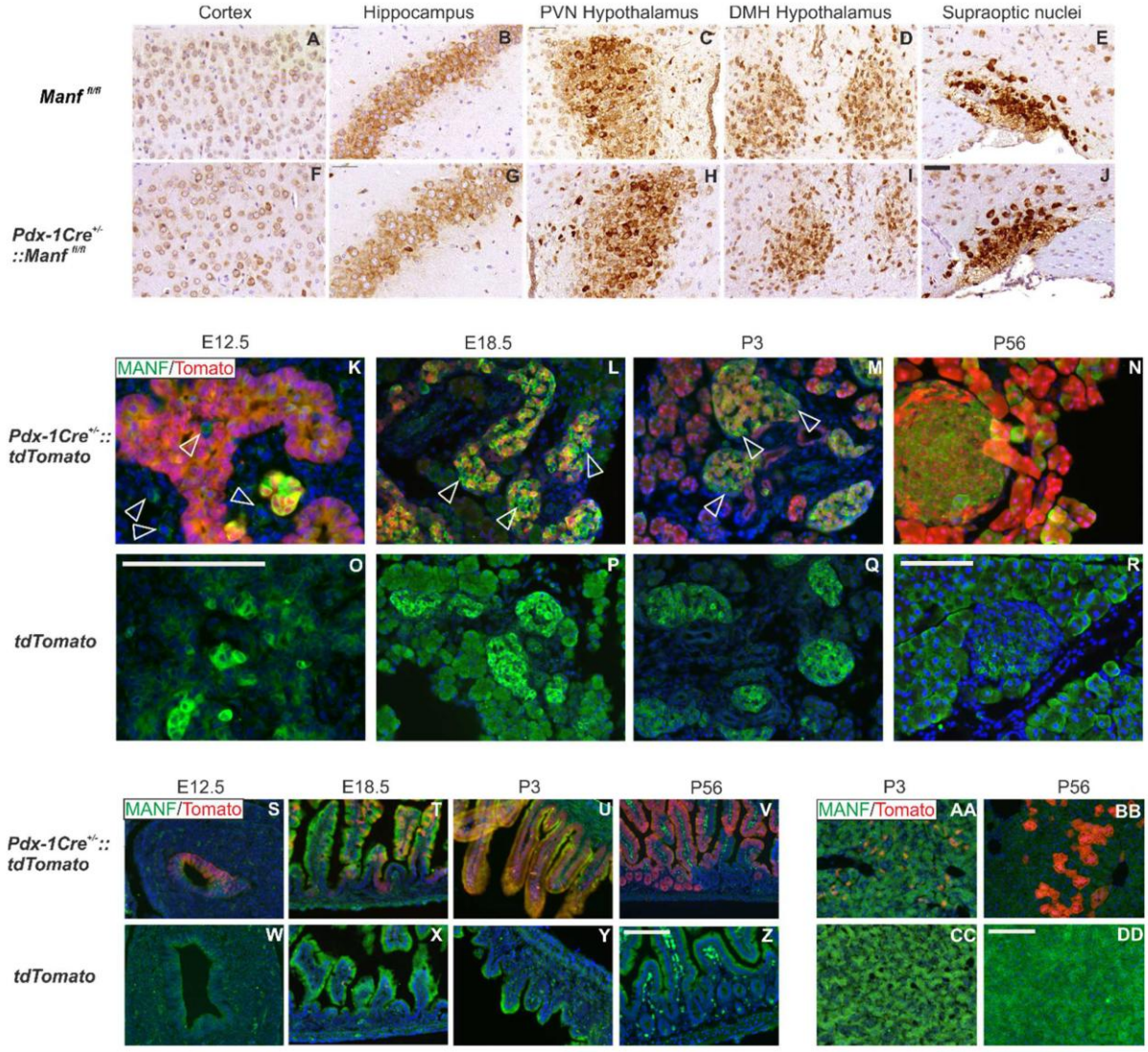

SUPPLEMENTARY DATA

Supplementary Figure 2.3. supporting Figure 2. MANF expression level in the pancreases of *Pdx-1Cre$^{+/-}$::Manf$^{fl/fl}$* mice is highly variable between individual mice

(A-I) Immunohistochemical peroxidase staining of MANF protein in *Manf$^{fl/fl}$* **(A, D, C)** and *Pdx-1Cre$^{+/-}$::Manf$^{fl/fl}$* **(B-C, E-F, H-I)** mice at P1 **(A-C)**, P14 **(D-F)**, and P56 **(G-I)**. Scale bar, 50 μm.

(J) Quantitative RT-PCR analysis for *Manf* mRNA levels in pancreatic islets isolated from *Manf$^{+/+}$*, *Manf$^{fl/fl}$* and *Pdx-1Cre$^{+/-}$::Manf$^{fl/fl}$* mice at P1 (n=6) , P14 (n=9) and P56 (n=10). *Manf* mRNA levels were significantly decreased in the islets of *Pdx-1Cre$^{+/-}$::Manf$^{fl/fl}$* compared to *Manf$^{fl/fl}$* islets. No difference in *Manf* mRNA expression levels was observed between *Manf$^{fl/fl}$* and *Manf $^{+/+}$* islets confirming that the remaining Frt-site and LoxP sites in the introns flanking exon 3 in the *Manf$^{fl/fl}$* gene does not disturb correct MANF pre-mRNA splicing and mRNA expression. Values represent mean ± SEM. *$p < 0.05$, **$p < 0.01$, ***$p< 0.001$.

(K-N) Immunoperoxidase staining of MANF protein in P1 *Pdx-1Cre$^{+/-}$::Manf$^{fl/fl}$* pancreas sections. MANF positive cells observed within the Langerhans islets **(L, N),** ducts and blood vessels **(M)** in the P1 pancreas of *Pdx-1Cre$^{+/-}$::Manf$^{fl/fl}$* mice. Scale bar, 50 μm, **(L-N)** Scale bar, 20 μm.

SUPPLEMENTARY DATA

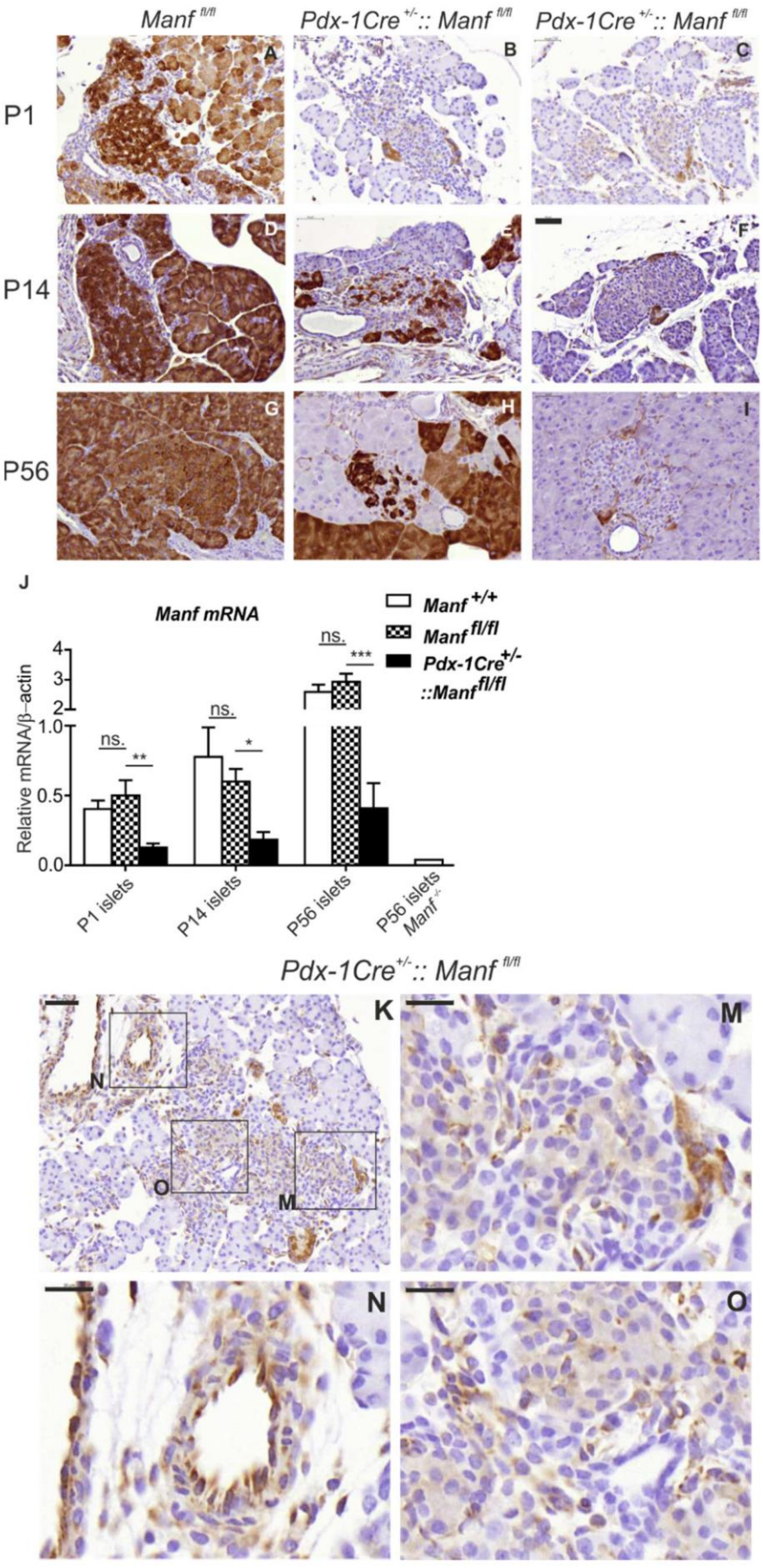

SUPPLEMENTARY DATA

Supplementary Figure 3. supporting Figure 3. Positive correlation of *Manf* mRNA with mRNA levels of β-cell specific genes and ultrastructural morphology of islet β-cells in 4-week-old *Manf*$^{-/-}$ pancreas.

(A-C) Positive correlation of *Manf* mRNA with *Pdx-1* ***(A)***, *Ins1/2* ***(B)***, *Glut2* ***(C)*** *mRNAs was observed between P56 Pdx-1Cre*$^{+/-}$::*Manf*$^{fl/fl}$ and *Manf*$^{fl/fl}$ mice. *n* =9-10 mice per group.

(D-G) Representative electron microscopy images of islets from 4-week-old *Manf*$^{+/+}$ **(D, E)** and *Manf*$^{-/-}$ **(F, G)** mice. Nucleus (N), endoplasmic reticulum(ER), secretory granule (SG), mitochondria (M). The loss of insulin secretory granules, enlarged mitochondria and dilated ER indicates ER stress-induced forthcoming β-cell demise in *Manf*$^{-/-}$ β-cells. Scale bar, 3 μm.

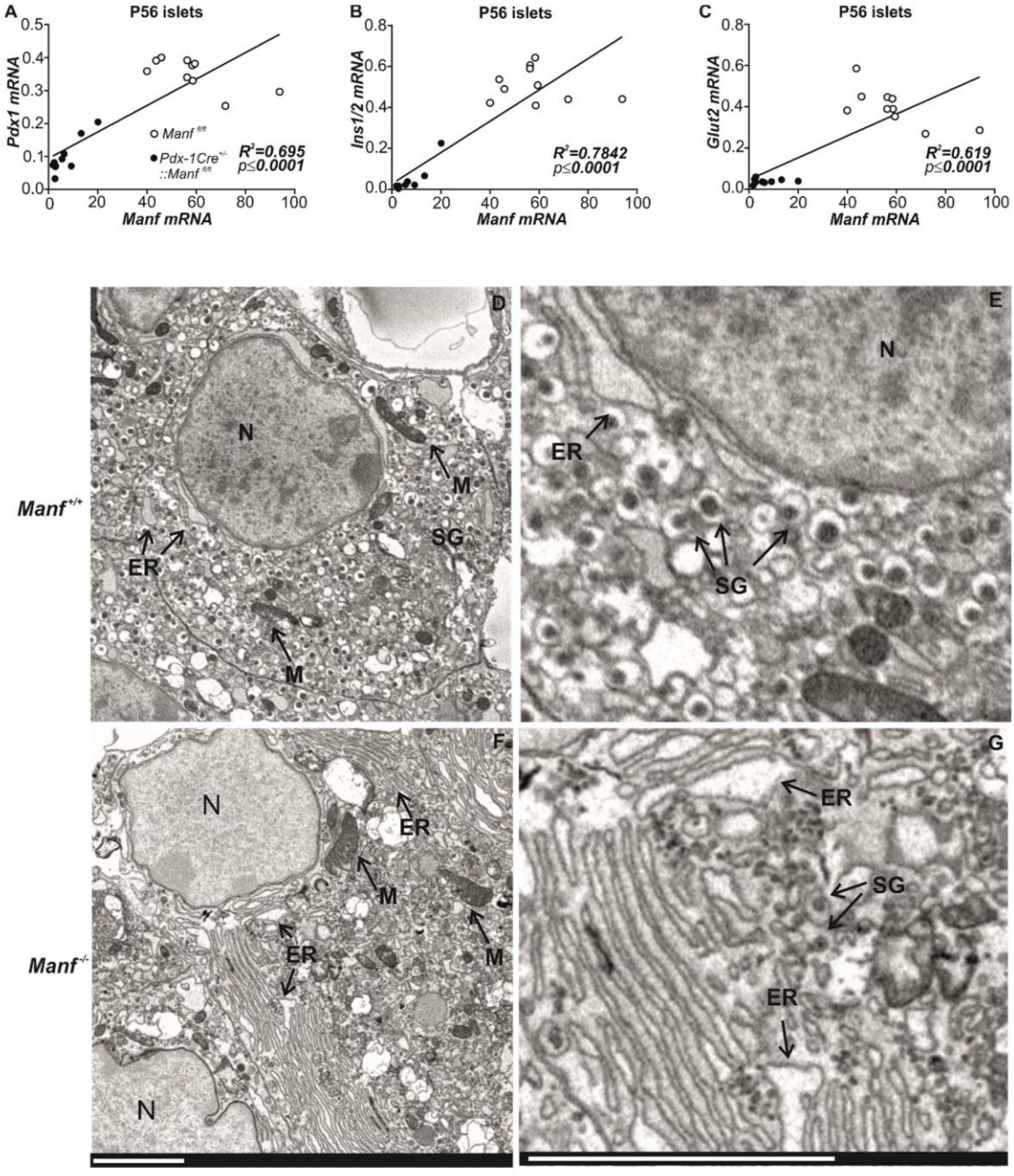

Supplementary Figure 4. supporting Figure 4. MANF induces proliferation of *Manf*$^{-/-}$ β-cells and reduces ER stress caused by MANF-deficiency in β-cells.

(A) Recombinant MANF protein at a concentration of 100 ng/ml increases proliferation of β-cells from 4-5-week-old *Manf*$^{-/-}$ mice after 5 days in culture. *n* =quantified from 4-7 wells per group.

(B) Quantitative RT-PCR PCR analysis of UPR genes *Atf4, Grp78, Chop, spXbp1, tXbp, Atf6a, Atf6β and of* β-cell marker *Glut2* from the isolated islets from 4-week-old *Manf*$^{+/+}$ and *Manf*$^{-/-}$ mice treated with 1 μg/ml human recombinant MANF overnight in 0.5% BSA medium. Human recombinant MANF is able to reduce ER stress in *Manf*$^{-/-}$ islets by downregulating UPR markers. *n* = 3-4 per group.

(C) Quantitative RT-PCR PCR analysis of UPR genes *Atf4, Grp78, Chop, spXbp1, tXbp, Atf6a, Atf6β and of* β-cell markers *Glut2, Pdx1 and Ins1/2* from isolated islets of 4-week-old *Manf*$^{+/+}$ and *Manf*$^{-/-}$ mice treated with 100 ng/ml human recombinant MANF for 3 days in 10% FBS medium. Human recombinant MANF is able to reduce expression levels of UPR markers *Chop* and *spXbp1* mRNA in isolated islets of *Manf*$^{-/-}$ mice. Additionally, a small but insignificant increase was detected in *Ins1/2* and *Pdx1* mRNA expression in *Manf*$^{+/+}$ islets treated with MANF for 3 days. *n* = 3-4 per group.

Values represent mean ± SEM. *p < 0.05, **p < 0.01, ***p< 0.001, ****p< 0.0001.

SUPPLEMENTARY DATA

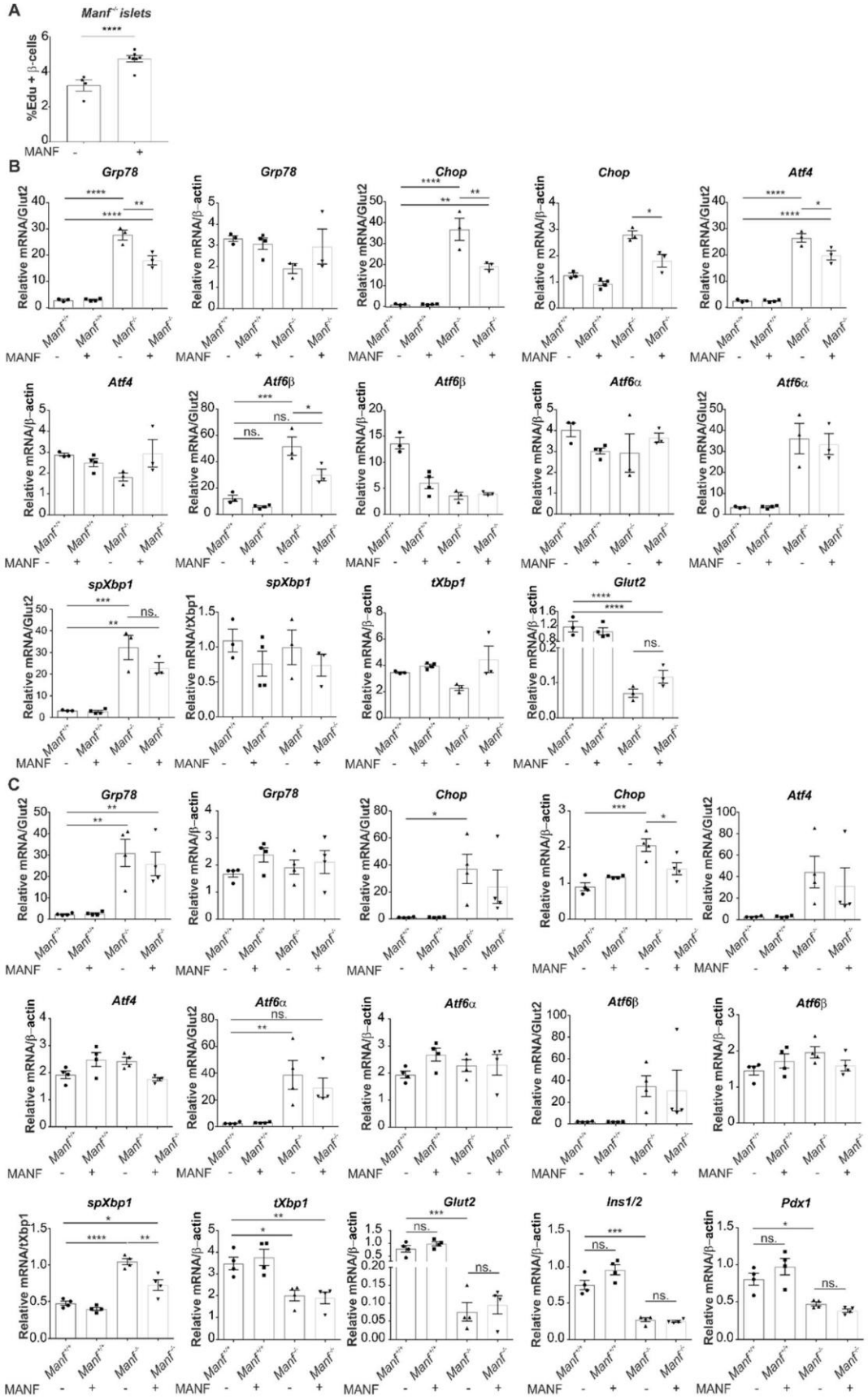

SUPPLEMENTARY DATA

Supplementary Figure 5.1. supporting Figure 5. MANF-deletion in adult β-cells results in reduced β-cell mass and diabetes *in vivo* in *MIP-1Cre^{ERT}::Manf$^{fl/fl}$* mice.

(A) Serum insulin levels measured 4 weeks after tamoxifen or oil injection from *ad libitum*-fed mice, *n* = 2-13 mice per group.

(B) Blood glucose levels measured after intraperitoneal glucose (2 g/kg) injection, *n* =2-12 mice per group.

(C) Blood glucose levels measured after intraperitoneal insulin injection (1 U/kg), *n* = 4-6 mice per group.

(D) Serum insulin levels measured from P90 mice 30 min after glucose bolus injection (2 g/kg), *n* =5-7 mice per group.

(E) Relative *Manf mRNA* levels in islets isolated from *Manf $^{fl/fl}$* mice injected with oil or tamoxifen and in islets from *MIP-1Cre^{ERT}::Manf$^{fl/fl}$* injected with oil or tamoxifen. *n* = islets from 7-9 mice per group.

(F-W) Immunohistochemical analysis of MANF **(F, I, L, O, R, U),** insulin **(G, J, M, P, S, V)** and glucagon-positive **(H, K, N ,Q ,T ,W)** cells in pancreatic sections reveals morphological changes in the islets of from *MIP-1Cre^{ERT}::Manf$^{fl/fl}$* injected with tamoxifen compared to control mice. Scale bar, 50 μm.

(X) The β-cell mass is significantly reduced in P90 *MIP-1Cre^{ERT}::Manf$^{fl/fl}$* mice injected with Tmx, compared to the β-cells mass in control mice, *n* = 2-6 mice per group.

(Y) The islet-cell mass quantified from Chromogranin A antibody-stained sections is significantly reduced in adult *MIP-1Cre^{ERT}::Manf$^{fl/fl}$* mice injected with TMX, compared to the islet-cell mass in control *MIP-1Cre^{ERT}::Manf$^{fl/fl}$* mice injected with oil, *n* = 5-6 mice per group.

(Z) α-cell mass in in P90 *MIP-1Cre^{ERT}::Manf$^{fl/fl}$* mice injected with Tmx, compared to the α-cell mass in control *MIP-1Cre^{ERT}::Manf$^{fl/fl}$* mice injected with oil , *n* = 5-6 mice per group.

Mean ± SEM, *p < 0.05, **p < 0.01, ***p< 0.001, ****p< 0.0001 versus the corresponding control.

SUPPLEMENTARY DATA

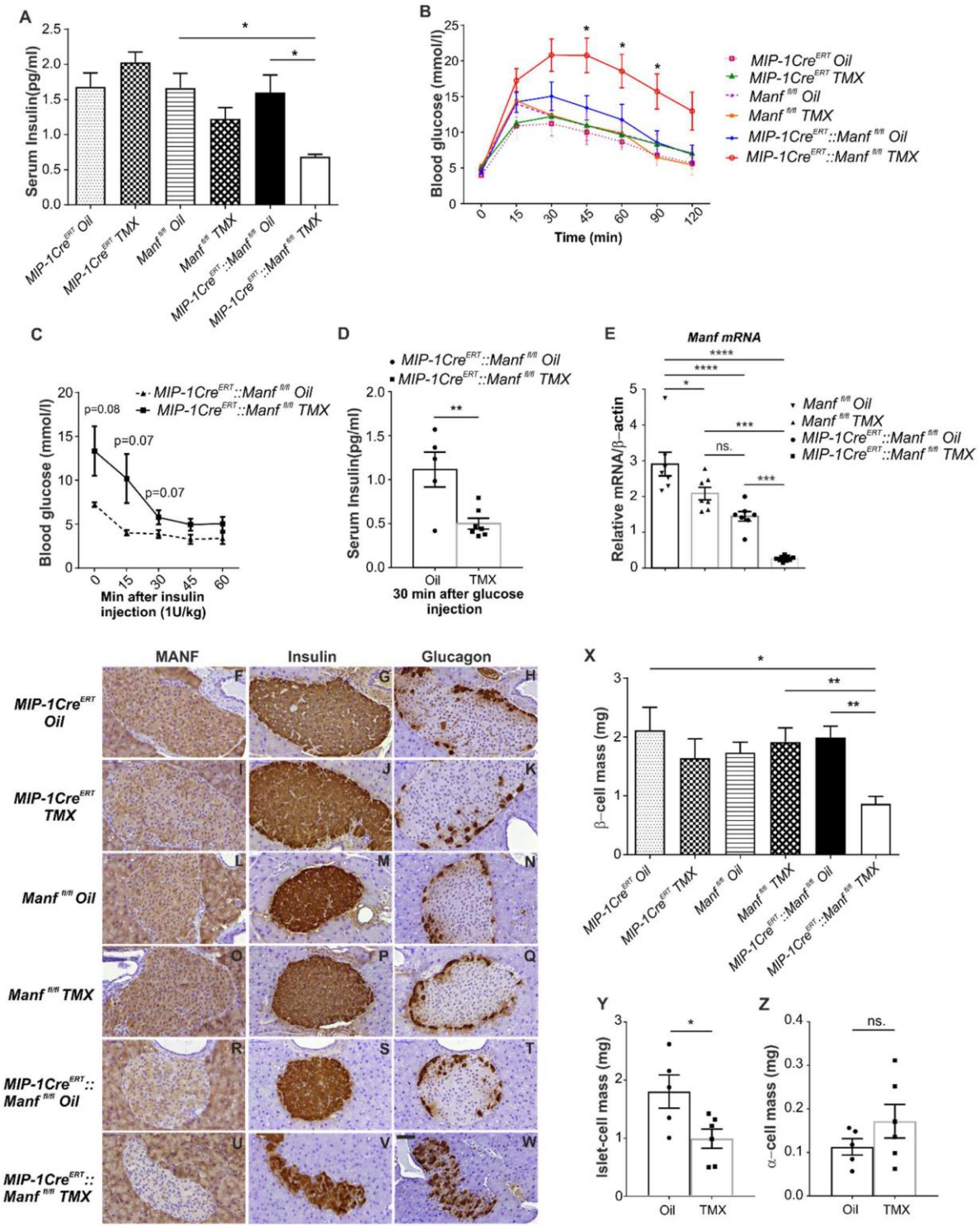

SUPPLEMENTARY DATA

Supplementary Figure 5.2. supporting Figure 5. MANF expression in the brain of *MIP-1Cre^{ERT}::Manf$^{fl/fl}$ mice.*

(A-J) Immunohistochemistry of MANF protein in brain sections from P90 oil-injected *MIP-1Cre^{ERT}::Manf$^{fl/fl}$(OIL)* **(A-E)** and tamoxifen-injected *MIP-1Cre^{ERT}::Manf$^{fl/fl}$(TMX)* **(F-J)**. No noticeable changes were detected in MANF expression in the cortex **(A, F)**, hippocampus **(B, G)**, paraventricular nuclei of hypothalamus (PVN) **(C, H)**, dorsal medial nuclei of hypothalamus (DMH) **(D-I)** and supraoptic nuclei of hypothalamus **(E, J)** between the different genotypes. Scale bar, 50µm.

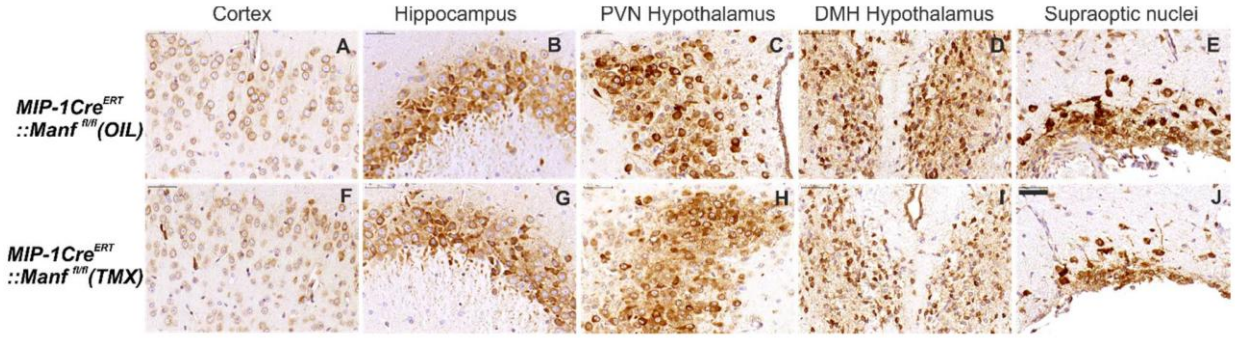

SUPPLEMENTARY DATA

Supplementary Figure 6. supporting Figure 7. Insights in the MANF mechanism of action

(A-B) Relative *Trib3* and *Bcl10 mRNA* levels in islets isolated from *Manf*$^{+/+}$ *and Manf*$^{-/-}$ mice at postnatal day 1 (P1) and P14. *n* = islets from 3-5 mice per group.

(C-G) Quantitative analysis of the western blot bands normalized to either total protein or GAPDH, *1.* *Manf*$^{+/+}$ islets, 2. *Manf*$^{+/+}$ islets cultured in the presence of 100 ng/ml of human recombinant MANF, 3. *Manf*$^{-/-}$ islets, 4. *Manf*$^{-/-}$ islets cultured in the presence of 100 ng/ml of human recombinant MANF. Mean ± SEM, *p < 0.05, ns., non-significant, of two independent experiments. *n* = 2-3.

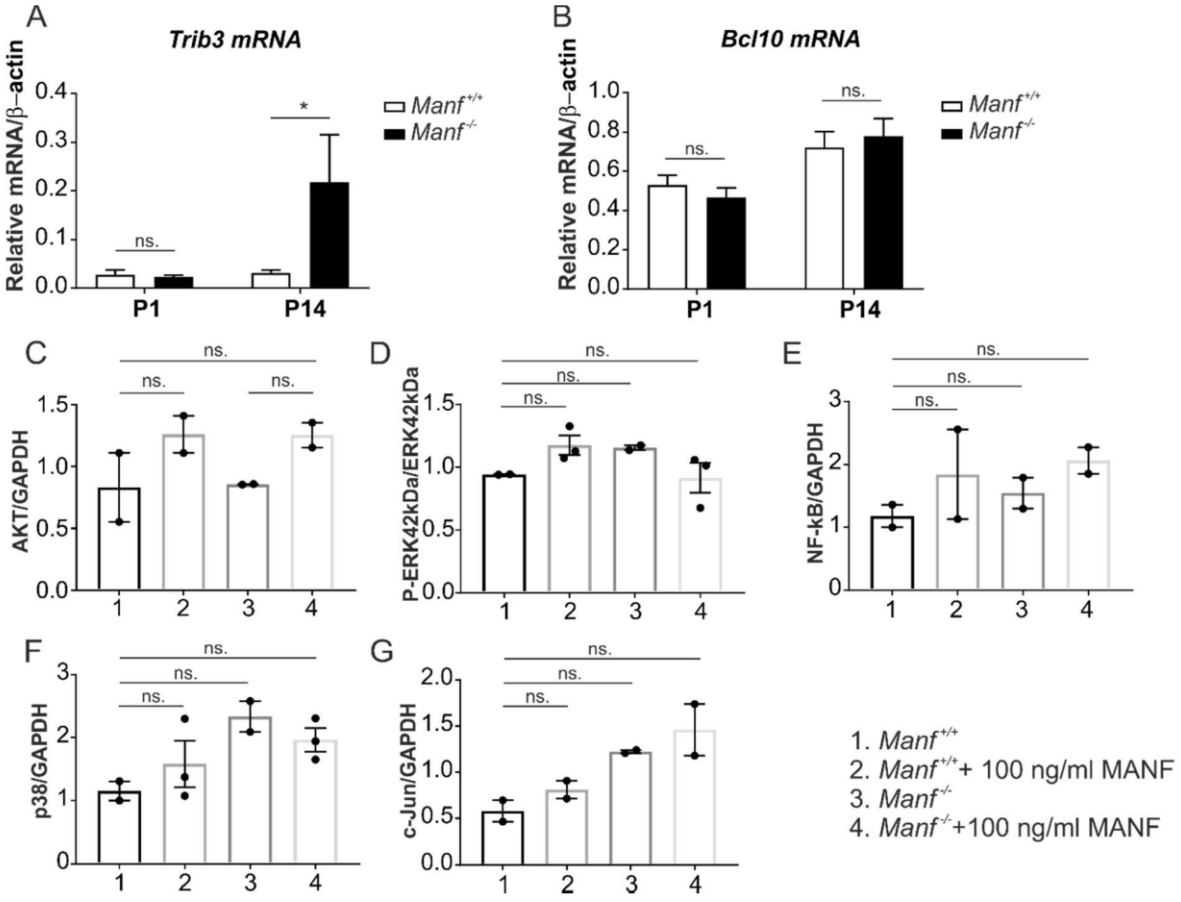

SUPPLEMENTARY DATA

Supplementary Table 1. Primary antibodies used in the study

Peptide/Protein target	Catolog number, Manufacture	Species raised in	Dilution	Country of origin
MANF	310-100, Icosagen	rabbit polyclonal	1:1000	Tartumaa, Estonia
MANF(ARP) C-19	sc-34560, Santa Cruz Biotechnology	goat polyclonal	1:500	Texas, USA
Insulin	ab7842, Abcam	guinea pig polyclonal	1:200	guinea pig polyclonal
Insulin	A0564, Dako	guinea pig polyclonal	1:2000	Santa Clara, California, US
Glucagon	ab10988, Abcam	mouse monoclonal	1:1000	Cambridge, UK
PDX1	07-696, Millipore	rabbit polyclonal	1:500	Billerica, Massachusetts, US
GLUT2	C-19, sc-7580, Santa Cruz Biotechnology	goat polyclonal	1:1000	Texas, USA
PP	A0619, Dako	rabbit polyclonal	1:600	Santa Clara, California, US
Somatostatin	A0566, Dako	rabbit polyclonal	1:200	Santa Clara, California, US
Ki67 (Clone SP6)	RM-9106, ThermoFisher Scientific	rabbit monoclonal	1:150	Waltham MA, USA
PDI	ADI-SPP-891-F, Enzo/AH Diagnostics	mouse monoclonal	1:200	Farmingdale, NY, USA
GM130	610823, BD Transduction Laboratories	mouse monoclonal	1:200	San Jose, CA, USA
GRP78(C-20)	sc-1051, Santa Cruz Biotechnology	goat polyclonal	1:500	Texas, USA
GAPDH	MAB374, Millipore	mouse monoclonal	1:3000	Billerica, Massachusetts, US
P-Akt	4058, Cell Signaling Technology	rabbit monoclonal	1:100	Danvers, MA, US
Akt	40D4,2920, Cell Signaling Technology	mouse monoclonal	1:500	Danvers, MA, US
P-p38	4631, Cell Signaling Technology	rabbit monoclonal	1:100	Danvers, MA, US
p-38	9218, Cell Signaling Technology	rabbit polyclonal	1:500	Danvers, MA, US
P-ERK1/2	E-4, sc-7383, Santa Cruz Biotechnology	mouse monoclonal	1:100	Texas, USA
ERK1/2	K-23, sc-153 Santa Cruz Biotechnology	rabbit polyclonal	1:500	Texas, USA
P-c-Jun	Ser63, 2361, Cell Signaling Technology	rabbit monoclonal	1:500	Danvers, MA, US
c-Jun	9165, Cell Signaling Technology	rabbit monoclonal	1:500	Danvers, MA, US

SUPPLEMENTARY DATA

Supplementary Table 1 continuation. Primary antibodies used in the study

Peptide/Protein target	Catolog number, Manufacture	Species raised in	Dilution	Country of origin
P-NF-κB	3033, Cell Signaling Technology	rabbit monoclonal	1:1000	Danvers, MA, US
NF-κB	8242, Cell Signaling Technology	rabbit monoclonal	1:1000	Danvers, MA, US
iNOS	M19, sc-650, Santa Cruz Biotechnology	rabbit polyclonal	1:500	Texas, USA
Chromogranin A	ab15160, Abcam	rabbit polyclonal	1:500	Cambridge, UK

Supplementary Table 2. Pearson´s correlation coefficient and Manders' coefficients for channel specific colocalization.

Slide name		Number of analysed cells	Pearson's coefficient Mean	Pearson's coefficient, Stderr	Mander's coefficient Mean	Mander's coefficient, Stderr
1	MANF	66	0.554	0.024	0.883	0.006
	ER				0.760	0.010
2	MANF	20	0.005	0.028	0.211	0.04
	Golgi				0.229	0.035
3	MANF	51	0.591	0.031	0.855	0.029
	Insulin				0.845	0.03
4	MANF	61	0.374	0.032	0.640	0.029
	GRP78				0.464	0.029